

Rethinking ion transport by ionophores: Experimental and computational investigation of single water hydration in valinomycin-K⁺ complexes

Eiko Sato^{1,2}, Keisuke Hirata^{1,2,4}, James M. Lisy^{*3,4}, Shun-ichi Ishiuchi^{*2,4,5} and Masaaki Fujii^{*1,2,4}

¹ *School of Life Science and Technology, Tokyo Institute of Technology, 4259 Nagatsuta-cho, Midori-ku, Yokohama, Kanagawa, 226-8503, Japan*

² *Laboratory for Chemistry and Life Science, Institute of innovative research, Tokyo Institute of Technology, 4259 Nagatsuta-cho, Midori-ku, 226-8503 Yokohama, Japan*

³ *Department of Chemistry, University of Illinois at Urbana-Champaign, Urbana, IL 61801, USA*

⁴ *Tokyo Tech World Research Hub Initiative (WRHI), Institute of Innovation Research, Tokyo Institute of Technology, 4259, Nagatsuta-cho, Midori-ku, Yokohama, Japan*

⁵ *Department of Chemistry, School of Science, Tokyo Institute of Technology, 2-12-1 Ookayama, Meguro-ku, Tokyo 152-8550, Japan*

Supporting Information

1. Experimental setup

Fig. S1 shows the experimental setup¹. Methanol solutions of valinomycin and potassium chloride were electrosprayed and the generated complex ions were introduced into a vacuum via a glass capillary heated to 60°C. The concentration of valinomycin and KCl were 10^{-5} M and 2×10^{-5} M respectively. The ions were guided to a clustering ion trap in which water molecules were introduced by a pulsed valve and micro-hydrate the ions. The clustering ion trap was cooled down to 70 K by a closed cycle He refrigerator. Hydrated complex ions of interest were mass-selected by a quadrupole mass spectrometer, deflected by a quadrupole bender and then guided into a cryogenic quadrupole ion trap (QIT.) The QIT was cooled to 4 K by a closed cycle He refrigerator. A mixture of hydrogen and helium buffer gas was introduced to the QIT via a pulsed nozzle and cooled down by collisions with the QIT's gold-coated copper electrodes. The complex ions were trapped and cooled to ~10 K by collisions with helium gas. Hydrogen molecules were condensed onto the cold ions, forming a variety of weakly-bound hydrogen cluster ions. The cluster ions were then irradiated with a tunable IR laser. Absorption of a photon resulted in the dissociation of the clusters, yielding the parent complex ion as a charged fragment. An IR absorption spectrum of the trapped ions was then generated by monitoring the fragment yield, recorded by a time-of-flight mass spectrometer as a function of the wavenumber of the dissociating laser light.

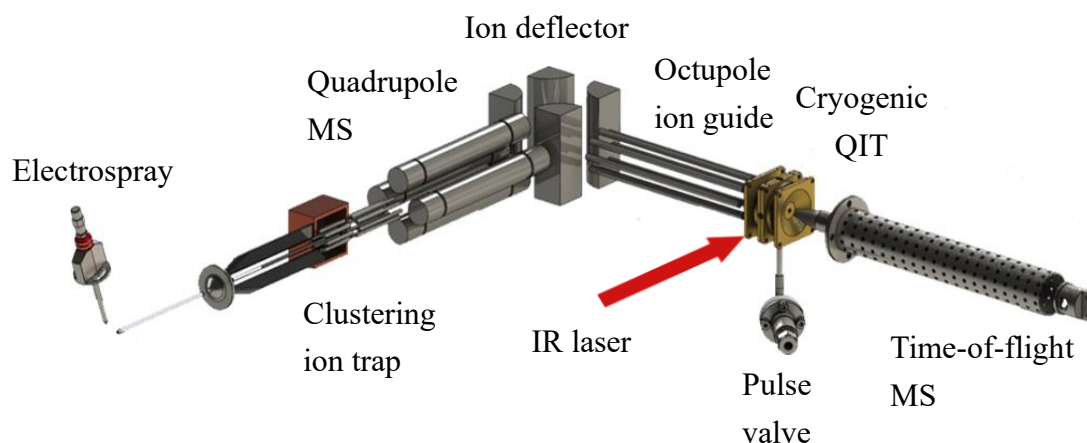


Fig. S1 Experimental setup

2. Computational details

Experimental vibrational frequencies tabulated in Tables S1 and S2 are taken directly from the spectra reported in Figures 2 and 3. Calculated vibrational frequencies presented in Tables S1 and S2 were obtained from DFT calculations using the dispersion-corrected B3LYP-D3BJ functional and the 6-31G(d,p) basis set². The DFT calculations were conducted using the Gaussian 16 package. Initial structures were prepared based on the geometry data of the crystal structure of K⁺-valinomycin (K⁺VM)³. A single water molecule was added to the NH, amide CO, and ester CO sites of (K⁺VM) from a number of varying orientations. To explore the potential energy surface and probe conformational energy barriers, the positions of the NH and CO groups were adjusted to stress the intramolecular NH \cdots OC hydrogen bonds and/or CO \cdots K⁺ distances. These initial structures of (K⁺VM)(H₂O), with the water positioned in locations above K⁺ on the Lac face, were subsequently optimized and the vibrational frequencies calculated. The three lowest energy conformers, designated K_A, K_B and K_C, with relative energies of 11.8, 12.0 and 0 kJ/mol respectively, had OH stretching frequencies that matched up well with the observed vibrational bands in that spectral region. As can be seen from Table S2, the frequency ordering of the three sets of OH stretches is consistent between the experimental and theoretical frequencies. In addition, the separations between the stretches (OH₁ and OH₂) for all three conformers are also a match (experiment:theory in cm⁻¹), 104:117, K_A, 160:163, K_B, 74:77, K_C. The calculated frequencies have been corrected for anharmonicity with a scaling factor (0.961), derived by averaging the ratio of calculated frequencies of the symmetric and antisymmetric stretches of H₂O at current level of calculation to the experimentally observed values⁴.

Table S1. Vibrational frequencies (cm⁻¹) for K⁺VM:

Experiment				Theory			
NH Stretch	Ester CO	Amide CO	NH bend	NH Stretch	Ester CO	Amide CO	NH bend
3289	1740	1653 1663	1546	3324 3339 3342	1730	1648 1661	1520 1535

Table S2. Experimental and calculated vibrational frequencies (cm^{-1}) for assigned $(\text{K}^+\text{VM})(\text{H}_2\text{O})$ conformers:

Assigned Conformer	Experiment		Theory	
	OH ₁ Stretch	OH ₂ Stretch	OH ₁ Stretch	OH ₂ Stretch
K _A	3564	3670	3520	3637
K _B	3548	3708	3538	3701
K _C	3591	3665	3610	3687

Structural comparison for K^+VM and the three $(\text{K}^+\text{VM})(\text{H}_2\text{O})$ conformers are compiled in Table S3. Distances from the calculations² were obtained using the Avogadro interface⁵. The average distance between K^+ and the three oxygen atoms of the ester carbonyl groups for the Lac and Hyv faces are given in the first two columns. The average hydrogen bond distance for the six amide groups and the distance between the water oxygen atom and K^+ for the three $(\text{K}^+\text{VM})(\text{H}_2\text{O})$ conformers are also provided. The uncertainties, one standard deviation, are in parentheses.

Table S3: Inter- and intra-molecular distances from the theoretical calculations.

Species	$\text{K}^+\text{-OC Lac}$ (Å)	$\text{K}^+\text{-OC Hyv}$ (Å)	NH-OC (Å)	$\text{K}^+\text{-OH}_2$ (Å)
K^+VM ($\text{C}_3 - \text{sym}$)	2.72	2.72	1.87(1)	N.A.
$(\text{K}^+\text{VM})(\text{H}_2\text{O})$ K _A	3.37(66)	2.61(1)	1.91(3)	2.68
$(\text{K}^+\text{VM})(\text{H}_2\text{O})$ K _B	3.54(1.36)	2.65(1)	1.93(4)	2.64
$(\text{K}^+\text{VM})(\text{H}_2\text{O})$ K _C	2.75(6)	2.69(2)	1.87(2)	3.85

Population estimates for the (K⁺VM)(H₂O) conformers in Table S4 were obtained from the area of the OH stretch bands, normalized by the vibrational transition moments from the DFT harmonic vibrational transitions⁶. The average of the OH₁ and OH₂ bands for each conformer were used to for the population estimates. The experimental vibrational frequencies for the specific conformers, the population estimates and calculated vibrational transition moments were used for the intensities to generated the vibrational spectrum for the individual conformers. The resulting combined fit is compared to experiment as shown in Figure S2.

Table S4: Calculated vibrational transition moments (VTM), integrated IR intensities (Int) and relative population (Ave Pop) of the (K⁺VM)(H₂O) conformers:

Species	OH ₁ VTM (arb)	OH ₂ VTM (arb)	OH ₁ Int (arb)	OH ₂ Int (arb)	Ave Pop (%)
K _A	216	530	0.335	2.34	18.5
K _B	228	291	0.734	2.67	10.9
K _C	68	281	4.73	7.65	70.6

Figure S2

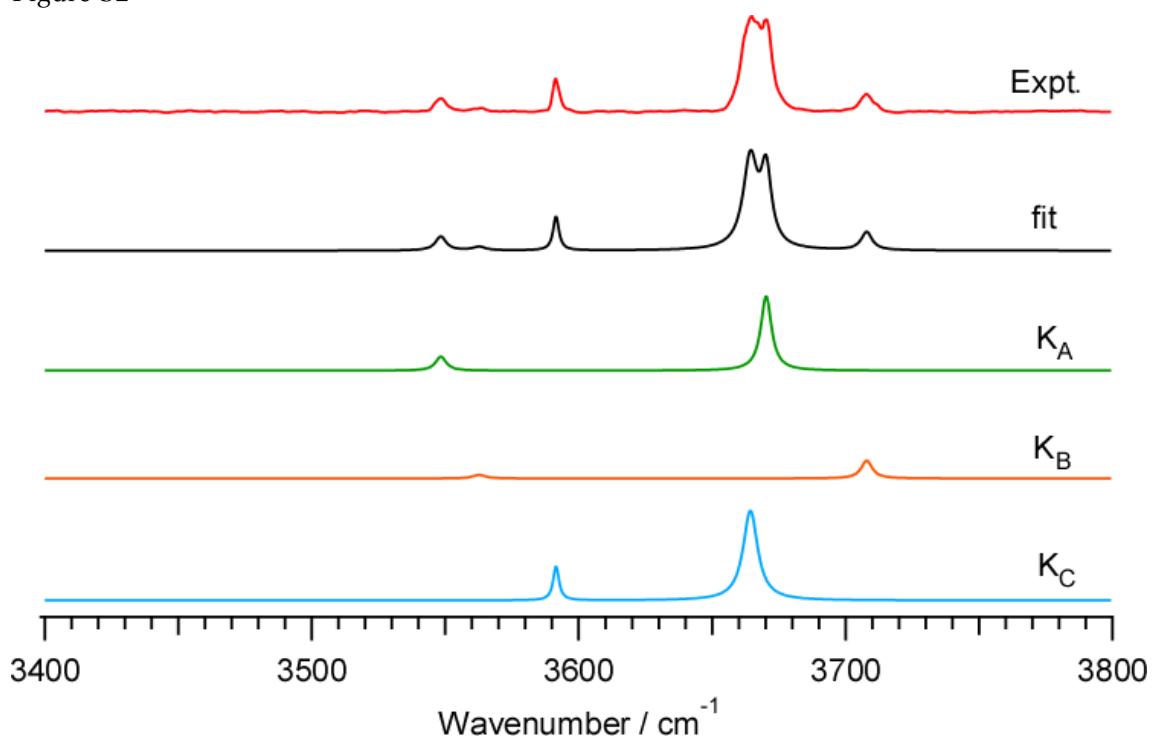


Figure S2. Calculated vibrational spectra for the individual conformers were obtained by first fitting the experimental band centers and peak heights to Lorentzian functions, which were then separated by conformer. The individual conformer integrated bands weighted by the calculated transition moments were then used to estimate the relative conformer populations.

References

- (1) Ishiuchi, S.; Wako, H.; Kato, D.; Fujii, M. High-cooling-efficiency cryogenic quadrupole ion trap and UV-UV hole burning spectroscopy of protonated tyrosine. *J. Mol. Spectrosc.* **2017**, *332*, 45-51.
- (2) Frisch, M. J.; Trucks, G. W.; Schlegel, H. B.; Scuseria, G. E.; Robb, M. A.; Cheeseman, J. R.; Scalmani, G.; Barone, V.; Petersson, G. A.; Nakatsuji, H.; Li, X.; Caricato, M.; Marenich, A. V.; Bloino, J.; Janesko, B. G.; Gomperts, R.; Mennucci, B.; Hratchian, H. P.; Ortiz, J. V.; Izmaylov, A. F.; Sonnenberg, J. L.; Williams; Ding, F.; Lipparini, F.; Egidi, F.; Goings, J.; Peng, B.; Petrone, A.; Henderson, T.; Ranasinghe, D.; Zakrzewski, V. G.; Gao, J.; Rega, N.; Zheng, G.; Liang, W.; Hada, M.; Ehara, M.; Toyota, K.; Fukuda, R.; Hasegawa, J.; Ishida, M.; Nakajima, T.; Honda, Y.; Kitao, O.; Nakai, H.; Vreven, T.; Throssell, K.; Montgomery Jr., J. A.; Peralta, J. E.; Ogliaro, F.; Bearpark, M. J.; Heyd, J. J.; Brothers, E. N.; Kudin, K. N.; Staroverov, V. N.; Keith, T. A.; Kobayashi, R.; Normand, J.; Raghavachari, K.; Rendell, A. P.; Burant, J. C.; Iyengar, S. S.; Tomasi, J.; Cossi, M.; Millam, J. M.; Klene, M.; Adamo, C.; Cammi, R.; Ochterski, J. W.; Martin, R. L.; Morokuma, K.; Farkas, O.; Foresman, J. B.; Fox, D. J. *Gaussian 16 Rev. C.01*, Wallingford, CT, 2016.
- (3) Neupert-Laves, K.; Dobler, M. The Crystal Structure of a K⁺ Complex of Valinomycin. *Helv. Chim. Acta* **1975**, *58*, 432-442.
- (4) Fraley, P. E.; Narahari Rao, K. High resolution infrared spectra of water vapor: ν_1 and ν_3 band of H₂¹⁶O. *J. Mol. Spectrosc.* **1969**, *29*, 348-364.
- (5) *Avogadro: an open-source molecular builder and visualization tool.*, 1.2.0.
- (6) Otsuka, R.; Hirata, K.; Sasaki, Y.; Lisy, J. M.; Ishiuchi, S.; Fujii, M. Alkali and Alkaline Earth Metal Ions Complexes with a Partial Peptide of the Selectivity Filter in K⁺ Channels Studied by a Cold Ion Trap Infrared Spectroscopy. *ChemPhysChem* **2020**, *21*, 712-724.